GRAVITY MODELLING OF THE LISCOMB 'SATELLITE' PLUTON

AN HONOURS THESIS

BY

MITCHELL BROGAN

April 14, 1988

Distribution License

DalSpace requires agreement to this non-exclusive distribution license before your item can appear on DalSpace.

NON-EXCLUSIVE DISTRIBUTION LICENSE

You (the author(s) or copyright owner) grant to Dalhousie University the non-exclusive right to reproduce and distribute your submission worldwide in any medium.

You agree that Dalhousie University may, without changing the content, reformat the submission for the purpose of preservation.

You also agree that Dalhousie University may keep more than one copy of this submission for purposes of security, back-up and preservation.

You agree that the submission is your original work, and that you have the right to grant the rights contained in this license. You also agree that your submission does not, to the best of your knowledge, infringe upon anyone's copyright.

If the submission contains material for which you do not hold copyright, you agree that you have obtained the unrestricted permission of the copyright owner to grant Dalhousie University the rights required by this license, and that such third-party owned material is clearly identified and acknowledged within the text or content of the submission.

If the submission is based upon work that has been sponsored or supported by an agency or organization other than Dalhousie University, you assert that you have fulfilled any right of review or other obligations required by such contract or agreement.

Dalhousie University will clearly identify your name(s) as the author(s) or owner(s) of the submission, and will not make any alteration to the content of the files that you have submitted.

If you have questions regarding this license please contact the repository manager at dalspace@dal.ca.

Grant the distribution license by signing and dating below.

Name of signatory	Date

ABSTRACT

The Liscomb 'Satellite' Pluton is a small granitoid mass located northwest of the main Liscomb Complex in central Nova Scotia. Detailed gravity data has been obtained over the smaller pluton , and from the surrounding area. Due to the density contrast that normally exists between intrusive bodies and their metamorphosed hosts it is possible to model the subsurface geometry of the intrusive body using Bouguer gravity data. The aim of this study has been to model the subsurface geometry of the Liscomb 'Satellite' Pluton and to establish its physical connection to the main Liscomb Complex.

During this study 96 gravity stations were surveyed over 22 km. with an average station spacing of 200 m. Over aproximately 11 km. of the survey gravity data was collected on a regional scale at a station spacing of 200 to 1000 m. Approximately 11 km. of the survey was conducted on, or in the immediate vicinity, of the Liscomb 'Satellite' Pluton using a station spacing of 100 to 200 m. In most cases the maximum amount of error associated with the Bouguer gravity values is ± 0.05 mgal.

Bouguer gravity contours show a -5.0 mgal. anomaly over the Liscomb 'Satellite' Pluton. Gravity modelling of this anomaly indicates that the pluton is an oval-shaped vertical cylinder with a convex upper surface. Results also indicate that the minimum depth extent of the pluton is 20 km., and that the pluton is connected to the main Liscomb Complex at a depth of 0.5 km. However, the connection between the pluton and the main Liscomb Complex does not appear to be consistant along the entire southern margin of the pluton.

TABLE OF CONTENTS

ACKNOWLEDGEMENTS

This study would not have been possible without the use of the equipment provided by various agencies, or their representatives. In this regards I would like to thank Dr. Tony Bowen of the Dalhousie University Oceanography Department for the use of the Omni Total Station surveying tool, as well as his assistants, Dave Hazen and Jay Deering, for their time and assistance in aiding me to understand the tool and use it properly. I would also thank Mike Hughes and the G.S.C. for the loan of their Lacoste-Romberg gravity meter. Most of all, I would like to thank my Honours Advisor, Dr. P. J. C. Ryall, for his time, valuable discussions, and advice throughout the duration of this study.

INTRODUCTION

The geology of central Nova Scotia consists of Devonian-Carbonifereous granites hosted by Cambro-Ordovician meta sediments. This study is concerned with the granitoid rocks of the Liscomb Complex and the associated gravity field. Figure 1 shows the regional geology surrounding the study area:

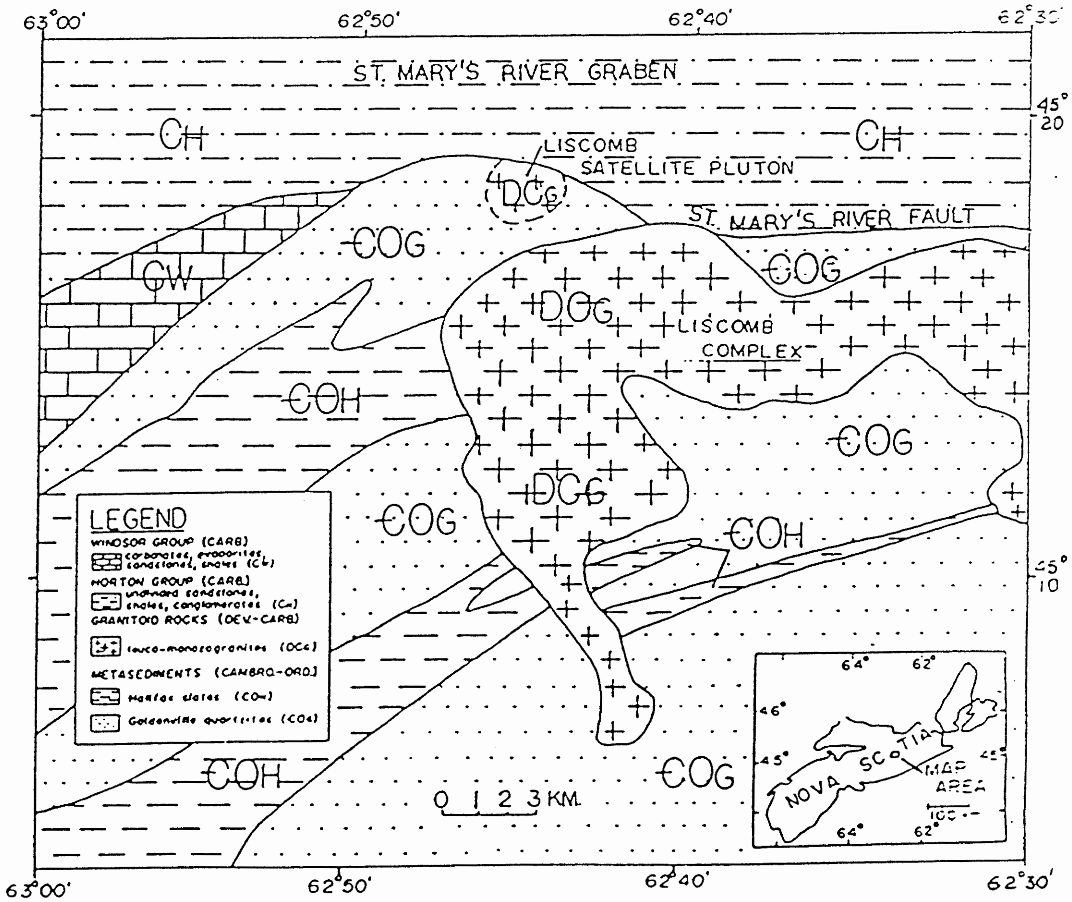

Figure 1, Regional geology of study area, located in central Nova Scotia (after Bujak and Donohoe, 1980).

The study area is located in central Nova Scotia just to the south of the St. Mary's River Graben (see fig. 1). The southern fault of the graben is the St. Mary's River Fault. The graben contains a veneer of Carbonifereous Horton Group (CH) sediments overlying the Cambro-Ordovician metasediments of the Halifax (€OH) and Goldenville (€OG) formations (Bujack and Donohoe, 1980). South of the St. Mary's River Fault are the granitoid rocks of the Liscomb Complex (DCG). As figure 1 shows, the granitoid rocks have intruded the Halifax and Goldenville formations. This study is concentrated on the small granitoid body (dashed contact) to the north of the main Liscomb Complex, which will be referred to in this study as the Liscomb 'Satellite' Pluton, and the associated gravity field.

As figure 1 shows, the boundary of the Liscomb Satellite Pluton has been inferred. Although the presence of the smaller pluton is illustrated on most geological maps of Nova Scotia, roadside surveying through the area failed to observe any outcrops. Initial gravity surveying (3rd year geophysics field school) indicated a decrease in the gravity field across the inferred contact. A detailed gravity study was conducted in order to model the subsurface geometry of the pluton. Such an interpretation would be useful to the study of granites in the area because the geometry of intrusive bodies is thought to have genetic significance (i.e., a dyke versus a pluton).

An important question in the study of granites involves the mode of emplacement of these bodies. Two important factors affecting the mode of emplacement of granite bodies are the geometry of the body and the net removal of mass during emplacement (Bott and Smithson, 1967). Work by Smith (1958) and Bott and Smithson (1967) have shown that gravity data can yield quantitative estimates of both the subsurface geometry of the granite body, and the missing mass.

Smith (1958) has shown that is possible to get quantitative estimates of a granite body's subsurface geometry using gravity techniques. Because most granite bodies have a negative density contrast with respect to the surrounding country rock there is normally a negative Bouguer gravity anomaly over the granite body. Talwani et al. (1959) provide a technique for approximating the subsurface geometry of a granite body to an n-sided polygon; and Nagy (1966) has shown that it is possible to approximate the subsurface geometry by a number of prisms. Bott and Smithson (1966) have investigated the missing mass problem and have concluded that at the very worst, gravity interpretations can be used to rule out certain mass distributions and associated hypotheses for emplacement. The reliability of such techniques depend on how well the rock densities are known and the precision of the gravity survey.

Previous gravity modelling of granite bodies in Nova Scotia has been done by Garland (1953), O'Reilly (1975), and Douma (1978). These workers were primarily concerned with modelling the largest body in Nova Scotia, the South Mountain Batholith. Douma (1978) had the largest database to work with. In plan view, his interpretation fit the general outline of the batholith as seen on geological maps of Nova Scotia. All three workers concluded that the batholith had a minimum thickness of 25 km.

Figure 2 is a schematic diagram showing the relationship between the regional Bouguer gravity contours and the surfacial geology of the study area. The associated Bouguer gravity minimum is typical of granite bodies in southern Nova Scotia. The contours of the diagram were derived from values contained in a regional database of gravity values maintained by Energy, Mines, and Resources (E.M.R.), Ottawa. Notable is the lack of expression of the Liscomb Satellite Pluton in the contours. This is attributed to the lack of data points around and over the smaller pluton.

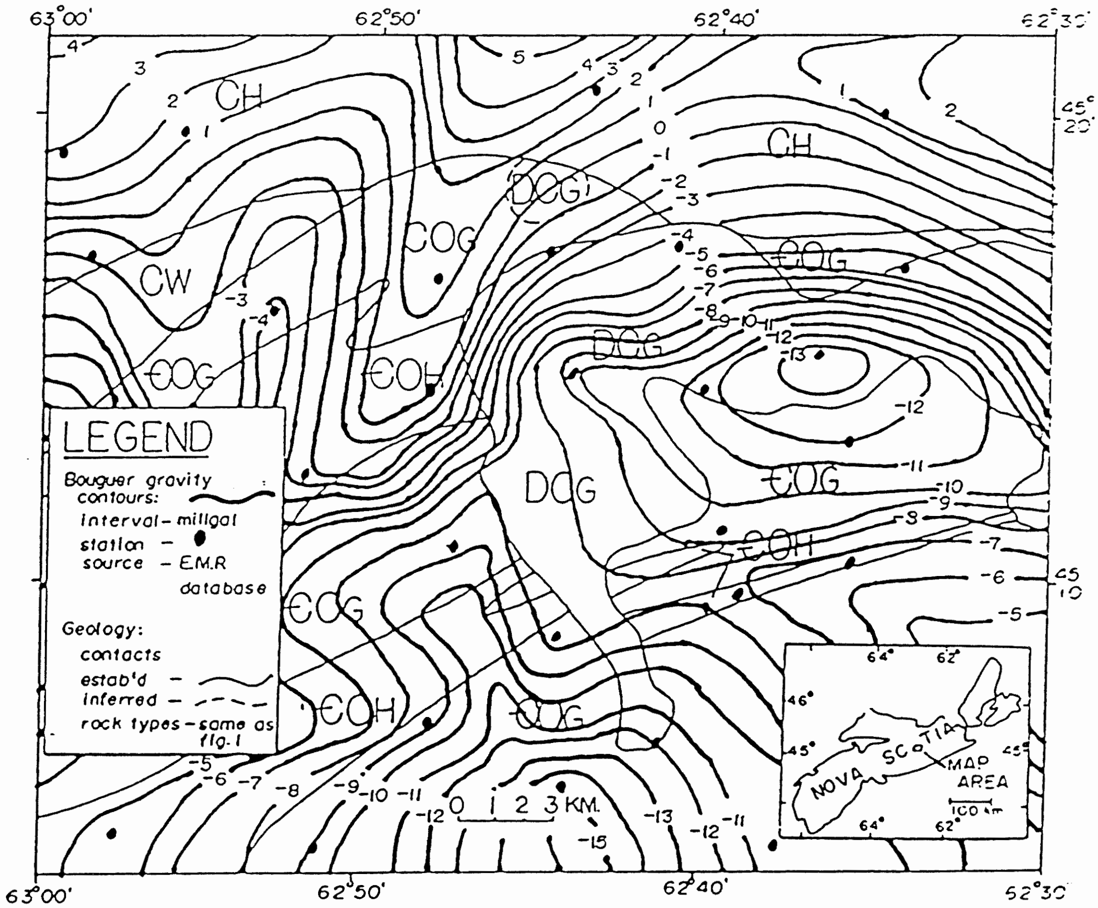

Figure 2, Schematic diagram showing the relationship between the regional Bouguer gravity contours and the regional geology.

All the previously published gravity studies in Nova Scotia were on a regional scale, and the spacing of the gravity stations is on the order of kilometers. In this study the data was collected on a detailed scale. It was thought that a detailed gravity survey over the Liscomb Satellite Pluton could yield a quantitative interpretation of the subsurface geometry, as well as provide reliable information regarding the mode of emplacement for the smaller pluton.

DATA ACQUISTION

Originally, the composition of the Liscomb Satellite Pluton was considered comparable to the composition of the main Liscomb Complex. However, reports by Giles and Chatterjee (1986, 1987) indicate that the composition of the main Liscomb Complex is quite complex. Figure 3 is a diagram showing the variety of rock types present within the main Liscomb Complex.

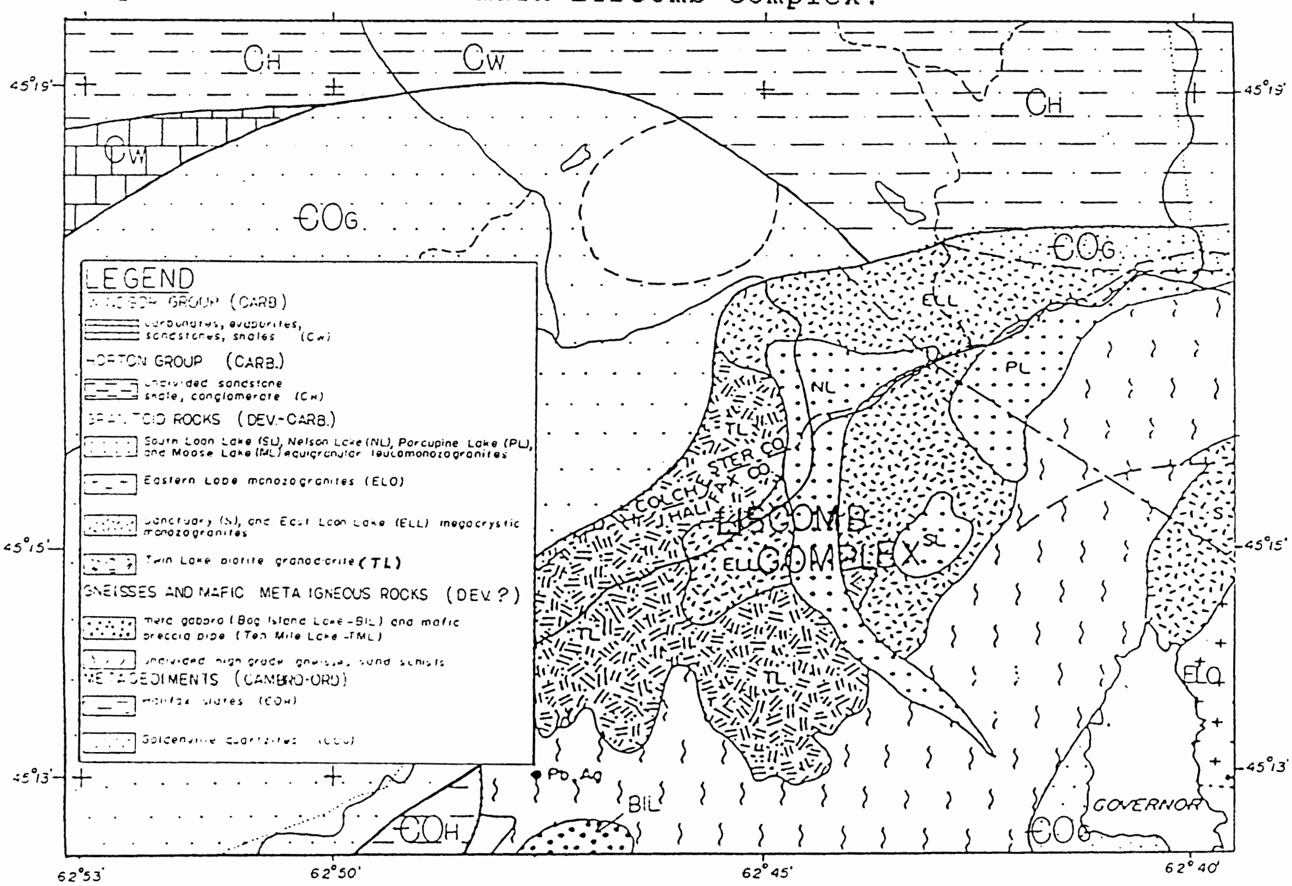

Figure 3. Updated geology of the northwest portion of main Liscomb Complex (after Giles and Chatterjee, 1987).

Once the complexity of the local geology was realized it became apparent that a better understanding of the regional gravity field was required to interpret a detailed gravity survey. This was because it was necessary to know how the gravitational effects of the main Liscomb Complex could affect the gravity of the Liscomb Satellite Pluton.

The best way to determine the regional gravity field around the Liscomb Satellite Pluton was to take gravity readings at known elevations. Figure 4 shows the map area and gravity stations used in this study.

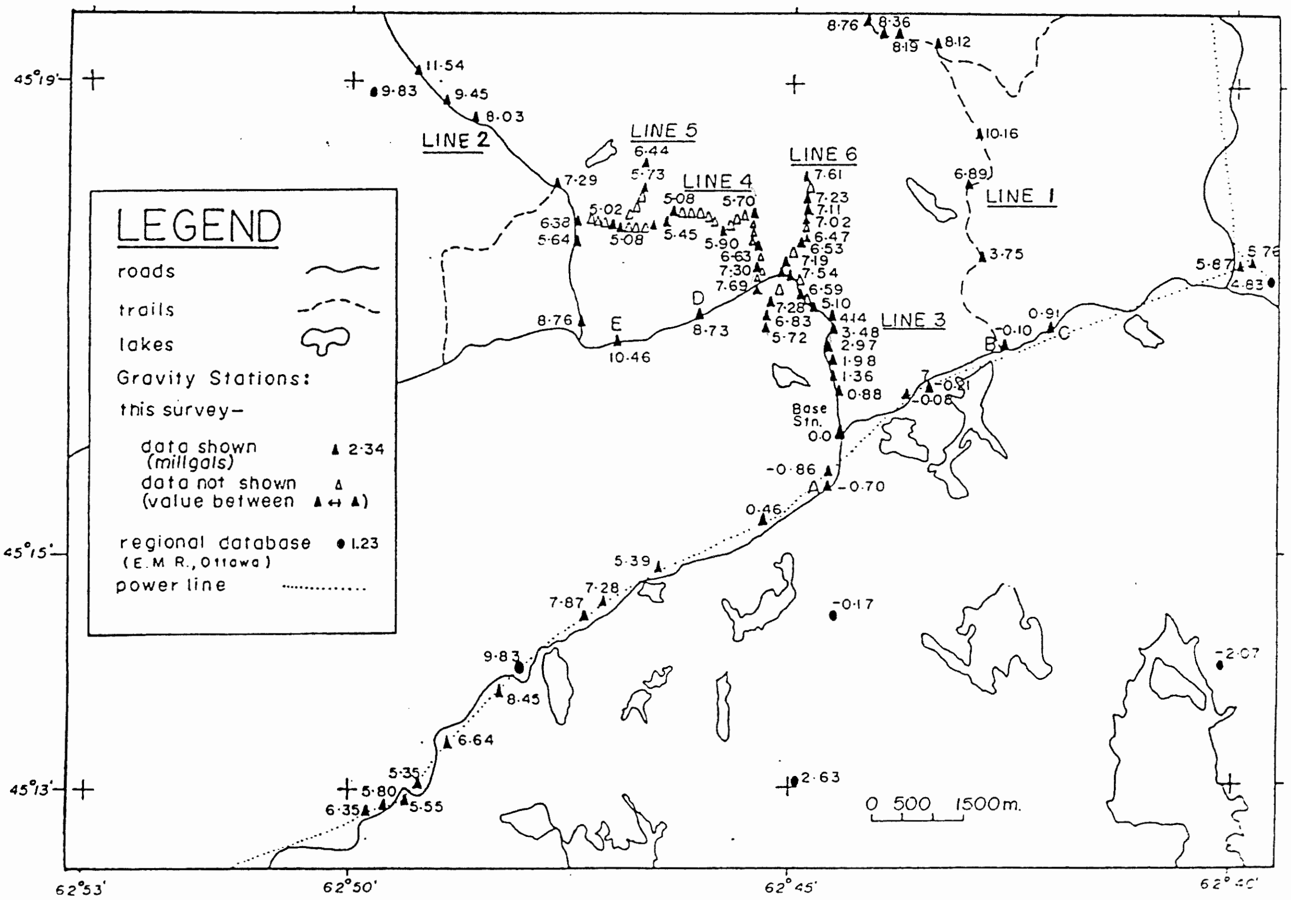

Figure 4 - Map area showing location of gravity survey lines and gravity stations.

In figure 4 the gravity stations along the power line (dotted line) were taken next to Nova Scotia Department of Lands and Forestry survey benchmarks. The gravity stations at A, B, C, D, E, Base station, and lines 1 and 2 were established at spot elevation positions read off orthophoto maps. The elevation of the Base station was later checked against a benchmark elevation.

Bouguer gravity values from these stations showed that the regional gravity field increases away from the main Liscomb Complex. Preliminary contouring showed the need for more data points between the Liscomb Satellite Pluton and the main Liscomb Complex. To rectify this problem, gravity stations were established along line 3 which follows the road north from the Base station and into the area of the Liscomb Satellite Pluton. These data points confirmed that the regional gravity field was increasing in value away from the main Liscomb Complex.

The results of the detailed gravity surveying indicated a depression in the gravity field over the inferred position of the Liscomb Satellite Pluton. Ideally, a gravity survey across the entire diameter of the pluton would have been desirable, but no road satisfying this condition could be found. However, two roads were found that crossed the inferred boundary of pluton: one from the south -line 4 , and one from the west - line 5. Along both roads the gravity values decrease to a minimum and then begin to increase towards the end of the line (see appendix A for description of start of lines and end of lines).

To increase the confidence in the gravity contours over the Liscomb Satellite Pluton more data points were required along the road south of the pluton (points D & E), and along a line that would cross the St. Mary's River Fault (line 6).

With the exception of the survey benchmarks and spot elevations all gravity stations were surveyed relative to the Base station using an Omni Total Station survey transit. This instrument uses a laser beam and three-cornered mirror to measure elevation changes and horizontal distances. The Omni Total Station has the capacity to take a number of readings and report the average value of those readings. The changes in elevation and horizontal distances surveyed for this study are the average of three readings.

Gravity measurements were made with a Lacoste-Romberg gravity meter. The Lacoste-Romberg gravity meter has a drift of 1.0 mgal./6 months, as claimed by the manufacturer. This feature increases gravity surveying considerably by not requiring frequent base station checks to correct for instrument drift. However, base station readings were taken approximately every 3.0 hours during gravity surveying.

DATA REDUCTION

Appendix A contains a table of all the gravity data including the raw data as well as all the corrections applied to obtain Bouguer gravity (B_grav) values for each station. In general, all corrections followed techniques outlined in Telford et al (1976). What follows is the procedure followed in this study to obtain Bouguer gravity values.

To obtain the observed gravity (G_obs) it was necessary to convert the gravity meter reading to milligals. The equation required to do this was:

$$G\_obs = [(s\_read - c\_read) * I\_F] + val\_mgal. \qquad (1)$$

where s_read is the station reading, the counter reading (c_read = 4000), interval factor (I_F = 1.06030), and value in milligals (val_mgal = 4231.51) were instrument dependent constants. Gravity readings taken following the first day required a base station correction (B_cor) which was used to correct every station with respect to the original base station reading. For some of the stations a temperature correction (T_cor) was required before calculation of the observed gravity. This temperature correction will be discussed in the next section.

Once the observed gravity was established a standard drift correction (D_cor) was applied to each station. The drift correction values between two base station values on the same day were calculated as follows:

$$D\_cor = [(Bstn_2 - Bstn_1) / t_{Bstn2}] * t_{stn} \quad (2)$$

where $Bstn_1$ was first base station reading, $Bstn_2$ was second base station reading, t_{bstn2} was number of minutes elapsed between taking the two base station readings, and t_{stn} was the amount of time elapsed since the first base station reading was taken and the reading of the station being corrected for instrument drift. Generally drift correction values for any individual station were very small (< 0.01 mgal/hr.), and probably represent tidal effects.

Latitude corrections of 0.8169 mgal/km. were applied which is consistent with a latitude of 45 degrees. The combined free air and Bouguer correction used was -0.193 mgal/meter assuming an average density of 2.63 $g/cm.^3$. All Bouguer gravity values in appendix A are relative to the base station. The general formula to obtain the Bouguer gravity (B_grav) is:

B_grav = G_obs + D_cor + L_cor + F_B_cor - Base_station (3)

L_cor is the latitude correction times the north - south distance (Dist) of the station relative to the base station. F_B_cor is the combined free air and Bouguer correction times the difference in elevation (D_el) between the station and the base station.

Although no EMR gravity stations were resurvyed during this study four stations were established near to EMR data points. In order to make the EMR data compatible with this survey the differences between the individual pairs were averaged and added to the EMR data points (9.76 mgal.). The EMR_C column in Appendix A gives the corrected values for this study's gravity gravity stations with respect to the EMR data base.

TEMPERATURE CORRECTION

Temperature variations can affect the gravity readings markedly. With the LaCoste-Romberg meter the effect of changing external temperatures is eliminated by running the meter at a constant temperature higher than any conceivable external temperature. A heater is built into the gravity meter and is powered by a battery pack. The manufacturer recommends that the gravity meter be at its internal operating temperature (49.5 C) for at least four hours prior to use. However, in the field, occassionally the battery pack and gravity meter would become disconnected because of a faulty connector, and the gravity meter's internal temperature would drop.

Such a temperature loss posed a serious question: does the instrument have to be at its recommended internal temperature for four hours before it is reliable again? This problem occurred twice during this study. The first time it occurred the instrument was allowed to reheat and surveying continued. This was early in the survey and the thinking was that the stations could, and would, be resurveyed. The second time the instrument suffered a temperature loss was late in the field season and resurveying would not have been possible.

To compensate for the temperature loss, the second time, the instrument was allowed to reheat to the recommended internal temperature and surveying did not continue until 20 minutes later. After the last station on the line was measured readings were continually taken at the base station and last station (0 E-N) until the gravity meter was deemed stablized. The gravity meter was considered stabilized when identical readings were obtained at the same station. Once stablization was clear second readings were taken at the first station (11 E-N), where the temperature loss occurred, and at an intermediate station (6 E-N).

day 1

station	1st reading	2nd reading	reading chg.	t (min.)
A	4084.270	4084.480	0.210	0
B	4079.480	4079.915	0.435	8
11907	4079.660	4079.863	0.203	27
19942	4080.790	4080.865	0.075	108
9995	4076.455	4076.485	0.030	131
day2				
11 E-N	4089.565	4090.420	0.855	20
6 E-N	4082.120	4082.860	0.740	58
0 E-N	4085.380	4085.425	0.045	125
Base stn	4079.895	4079.930	0.035	144

Table 1 : Temperature loss data. The first reading is the reading during the instability period of the gravity meter. The second reading is the reading from the same station after the gravity had stabilized. The change in readings is the second reading minus the first reading.

Time (t) is the time between when the instrument suffered its temperature loss and when the first reading at that station was taken. Data in milligals.

The logic of this procedure was that if the stability of the instrument was a function of temperature then a plot of the change in readings with time would yield a correction curve. Basically, the resultant curve would be a 'drift' correction curve. Figure 5 is a plot of the data contained in table 1:

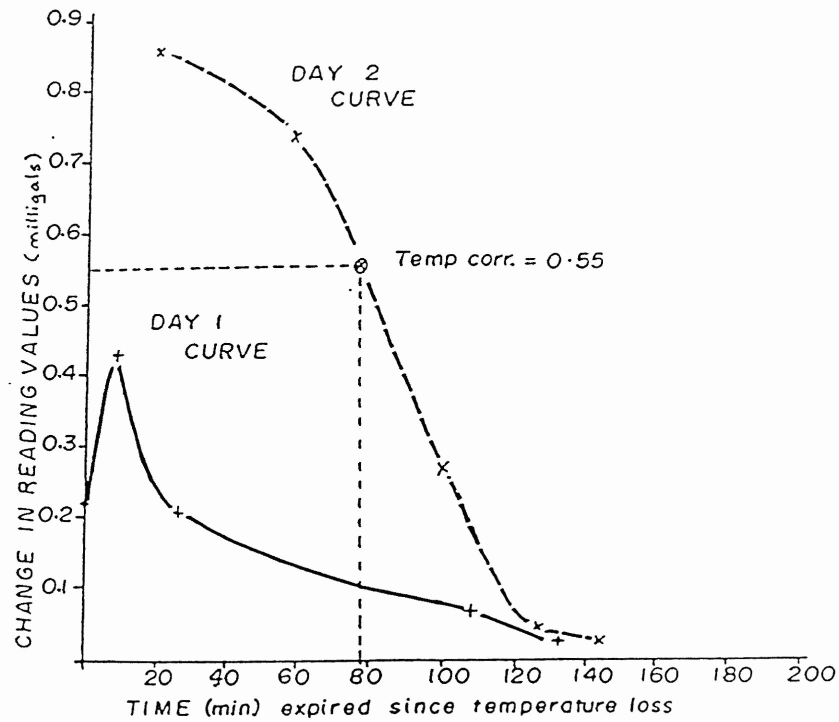

Figure 5 : Temperature correction curves for day 1 and day 2. Only the curve for day 2 is used as a correction curve because day 1's stations were resurveyed. Day 1's curve is included here only for comparison.

The curve for day 1's data shows that initially the instrument is quite erratic, but tends to smooths out with time. The curve for day 2's data does not show the initial erratic behavior, but similar to day 1's curve it smooths out with time. Although the slopes of the curves are different they both show a decrease in the difference between the readings implying that the instrument is stabilizing. The two curves merge at about 125 minutes suggesting that the instrument required about this much time to stabilize. The difference in the slopes of the two curves and the magnitude of the differences in readings can be attributed to the magnitude of the initial temperature loss which was greater on day 2.

ERROR ESTIMATES

In this study there are three major sources of errors: the ability to repeat a gravity reading, changes in elevation measurements, and horizontal distance measurements.

The precision of the gravity meter is ± 0.001 mgal. To determine the ability to repeat a measurement the gravity meter was set-up in a stable location and several readings were taken. This procedure indicated that a reading could be reproduced only to ± 0.01 mgal. Thus, the accepted error associated with reading the gravity meter is ± 0.01 mgal.

The changes in elevation measured using the Omni Total Station are actually the mean value of three successive readings. Observation of the Omni Total Station during surveying found an error of ± 0.001 m. associated with each station. Theoretically, these errors accumulate with successive measurements away from the known elevation. Standard procedures for the treatment of experimental errors state that the cummulative error is equal to the square root of the sum of the individual errors squared.

The maximum error due to errors in elevations will be coincident with the last station of line 4 which is the maximum number (36) of measurements away from a known elevation. Therefore, the maximum cummulative error due to elevation errors is ± 0.006 m. This translates to a maximum error contribution of ± 0.001 mgal. in the combined free air and Bouguer correction due to errors in changes of elevation measurements for stations surveyed using the Omni Total Station. Elevation errors associated with the benchmark elevations are probably insignificant; however, the spot elevations are probably only known to ± 0.5 m. Such an error would translate to an error in the gravity readings for these stations of ± 0.1 mgal.

To determine the north-south distances relative to the base station each station location was plotted on a 1:50,000 scale map, and extrapolated to a north-south perpendicular through the base station. The north-south distances were then measured along the perpendicular and converted to metres. The horizontal distances were also measured using the Omni Total Station. According to the Omni Total Station operation manual the distances have an error of ± 0.005 m./reading.

Following the same procedure as for the cummulative error in the elevation changes yields a maximum cummulative error of ± 0.03 m. in the horizontal distances. On a scale of 1:50,000 this error is insignificant; however, measuring the actual north-south distances to ± 0.001 m. on a scale of 1:50,000 converts to a real error in the north-south distances of ± 50 m. Using a latitude correction of 0.000817 mgal./m. leads to an error contribution of ± 0.04 mgal. due to errors in horizontal distances.

Because of the nature of applying corrections to gravity data the combining of individual errors is similar to the equation for determining the cummulative error of a series of measurements such that:

$$\text{error\_BG} = [A^2 + B^2 + C^2]^{1/2} \qquad (4)$$

where A is the error contribution due to the inability to repeat a measurement (=±0.01 mgal.), B is the error contribution due to elevation measurements (± 0.001 mgal.), C is the error due the horizontal measurements (± 0.04 mgal.), and error_ BG is the maximum error in the Bouguer gravity values. Solving this equation gives a maximum error of ± 0.05 mgal. associated with each gravity station except for the stations established at spot elevations where the error is ± 0.1 mgal.

RESULTS

A contour map of the Bouguer gravity over the area of the Liscomb Satellite Pluton is presented in figure 6. The contour map shows a depression in the gravity field associated with the Liscomb Satellite Pluton. Assuming a background of 10 milligals, the gravity contours in figure 6 show a negative anomaly of 5.0 mgal. over the area of the Liscomb Satellite Pluton, and a - 12.0 mgal. anomaly associated with the main Liscomb Complex.

The interpretation of the negative gravity anomaly associated with the Liscomb Satellite Pluton involved finding the subsurface shape which best reproduced the Bouguer gravity values along the three profiles shown in figure 6. The profiles were chosen so that their intercept was at 'C', which was taken to be the centre of the anomaly. Interpretation involved using a 2.5D gravity modelling program called Magrav , as well as a 3D gravity modelling program called Threed.

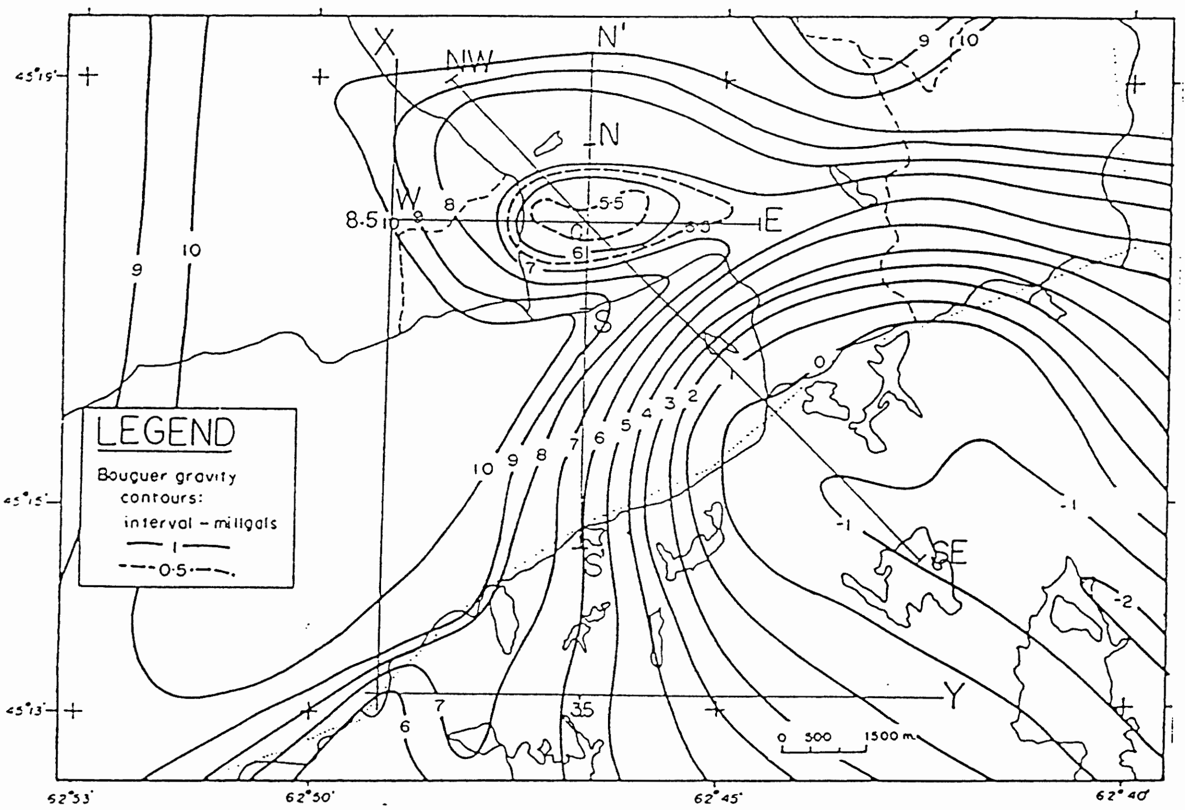

Figure 6: A contour map of the Bouguer gravity values for the area of the Liscomb Satellite Pluton. Note the depression in the gravity field over the Liscomb Satellite Pluton.

Magrav is a computer program based on techniques derived by Talwani et al (1959). The technique involves approximating the subsurface geometry by an n-sided polygon, and calculating the resultant gravity effects along a profile crossing the width of the anomaly. Modelling requires the adjustment of the polygon's dimensions until the calculated gravity profile matches the observed gravity profile.

The original mathematical formula derived by Talwani et al

(1959) assumed an infinite strike length perpendicular to the profile direction. By specifying a limited half-strike length the Magrav program can correct for end effects. In real terms, if the length to width ratio is greater than 10 to 1 the infinite strike length approximation is not a bad one. Unfortunately, the anomaly over the Liscomb Satellite pluton has a length to width ratio of approximately 3 to 1. This ratio limits modelling to only the N-S profile using Magrav.

Program Magrav requires that the interpreter specify certain parameters to be used in the calculation of the gravity effects. These parameters are: the density contrast between the body and the surrounding rock; the half-strike length of the body perpendicular to the profile line; the spacing between the points of calculation along the profile; and the initial co-ordinates of the polygon's corners. Ideally, these values should be based on data independent of the gravity data so that the interpretation is not soly based on gravity data

The density contrast used for this model was - 0.09 g/cm^3. This value is based on the average densities of the Meguma metasediments (2.73 g/cm^3) and the granitoid rocks (2.64 g/cm^3) found in Nova Scotia (Douma, 1978). Although the density values can vary considerably within either rock group the values used here are justified on the basis of the local geology. In the modelling programs used for this study the density contrast acts as a scaling factor which will be discussed later.

The half-strike length parameter for each profile was based on the inferred limits of the Liscomb Satellite Pluton as shown on geological maps of the area. The spacing of the calculation points along the profiles was set at 0.25 km. Depth to top of the body is assumed to be zero because the geological maps show the Liscomb Satellite Pluton to be outcropping.

Figure 7A shows the comparison of the observed gravity values and the calculated gravity values based on the subsurface body shown in figure 7B.

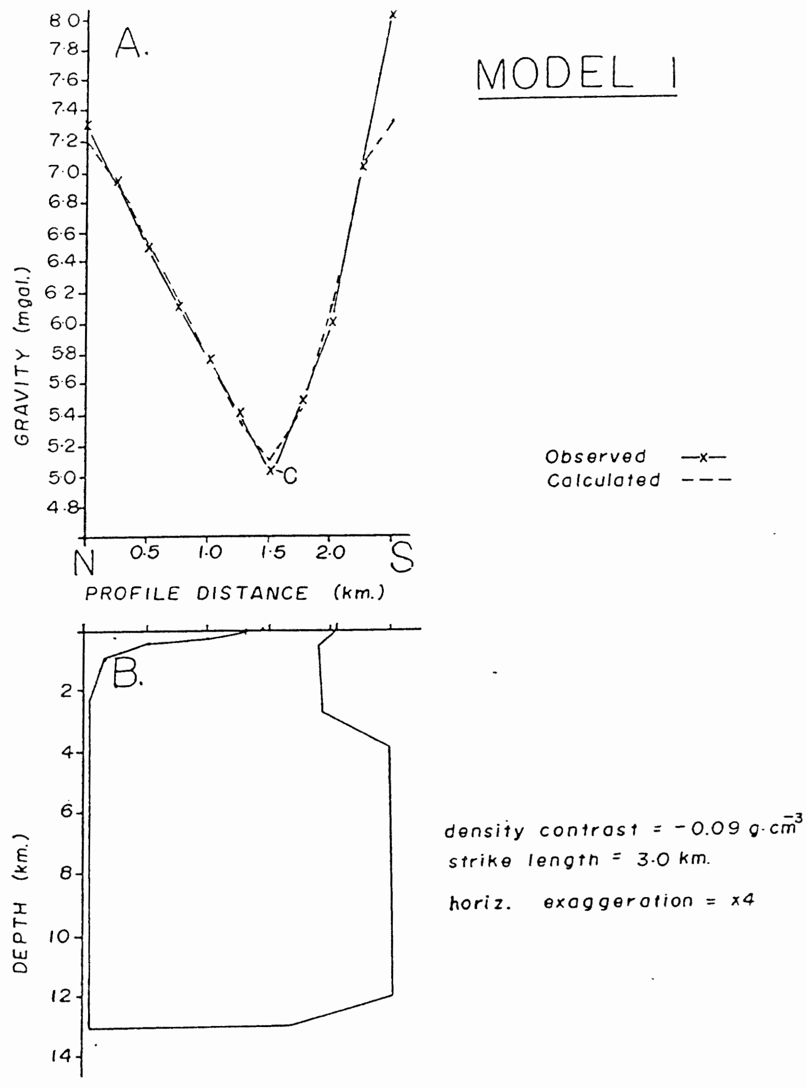

Figure 7 : A schematic diagram showing the best-fitting model calculated using the program Magrav along the N-S profile of figure 6. Note this profile is shorter than the N'-S' profile.

Figure 7B shows a body extending to a minimum depth of 13.0

km. The minimum profile width of the body is 2.5 km. The half-strike length used in the calculations was 1.5 km. yielding a total strike-length of 3.0 km. The noteworthy features of this model are the steeply sloping contacts, the lack of physical contact with the main Liscomb Complex to a least a depth of 13.0 km., and the poor fit between the calculated and observed curves towards the south in figure 7A.

The calculated profile in figure 7A shows a problem with modelling the Liscomb Satellite Pluton. At the southern end of the profile in figure 7A the calculated gravity is going less positive than the observed gravity. The effect of the main Liscomb Complex, which lies to the southeast, would be to cause the calculated gravity to become more negative. This is because the main Liscomb Complex also has a negative density contrast, according to the regional gravity contour map (figure 2). The implication is that a density contrast of -0.09 g/cm^3 is not great enough to produce a calculated anomaly of the same magnitude as the observed gravity anomaly. Consequently, it was necessary to find the value of the density contrast that could be used to produce a calculated anomaly similar in magnitude to the observed gravity anomaly. A 3D gravity modelling program, called Threed, was used to find the approximate mass distribution of the pluton by incorporating a first-order approximation to the effect of the main Liscomb Complex in the modelling.

Threed is a 3D gravity modelling program based on a technique developed by Nagy (1966) to calculate the gravitational effect of a right rectangular prism, or block. Gravity modelling with Threed involves approximating the subsurface geometry of the body by n-number blocks whose sides are parallel to an arbitrary X-Y coordinate system. The X-Y coordinate system used in this study is shown in figure 6.

The program Threed requires that the corners (X_1, X_2, Y_1, Y_2) of each block be specified with respect to the arbitrary X-Y coordinate system. The interpreter must also specify the depth to the top of each block, as well as the depth extent of each block. The interpreter must be careful to ensure that the blocks do not overlap, or that there are no unwanted gaps between the individual blocks. The program calculates the gravitational effect of each block separately then sums the gravitational effect of all the blocks for a point of calculation specified relative to the X-Y coordinate system.

The program Threed can produce gravity values for a single point, a series of points along a profile, or a grid of points. The interpreter must specify the points of calculation with respect to the X-Y coordinate system. For example, to get the calculated gravity values along the N-S' profile shown in figure 6, X was choosen to be 12000 and Y was set at 3500. Then the spacing of the calculation points (DX) was set to 500 and the number of points along the profile at which calculation was to be done was set at 20. This resulted in 20 values spaced 500 m. apart along a profile line starting at X = 12000 and ending at X = 2000 with Y = 3500.

Once the output from the program was obtained the values were plotted at the appropriate scale and compared to the corresponding observed gravity profile. Modelling was done by adjustment of the blocks until there was good agreement between the calculated and observed gravity profiles. Figure 8 shows the results of modelling along the three profiles, N'-S', W-E, and NW-SE.

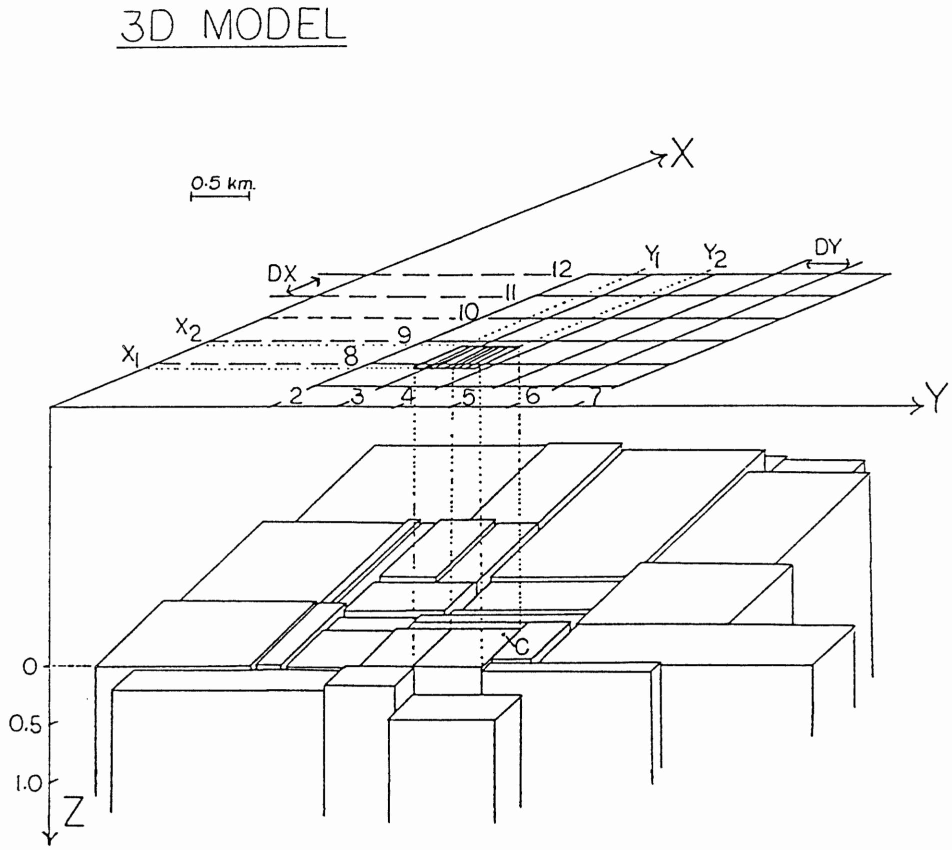

Figure 8. A schematic diagram showing the 3D geometry of the Liscomb Satellite Pluton resulting from 3D gravity modelling using the program Threed. The notations used in the diagram are explained in the previous discussion. All blocks extend to a depth of 20 km.

The best-fit model shown in figure 8 approximates the Liscomb Satellite Pluton by 30 vertical blocks. The boundaries of the individual blocks should be regarded as approximate. The 3D model produced indicates that the Liscomb Satellite Pluton is probably oval-shaped in plan view. The figure caption shows that the pluton extends to a minimum depth of 20 km. The body has a north-south length of approximately 3.5 km. and a east-west length of 4.0 km. The model shows that the pluton slopes gradually to the east, west, and north from 'C', whereas the southern contact of the pluton is very steep. Although the eastern, western, and northern contacts of the pluton slope gradually at first they become very steep at a distance away from 'C'. This model suggests that the pluton is an oval-shaped vertical cylinder with a convex upper surface.

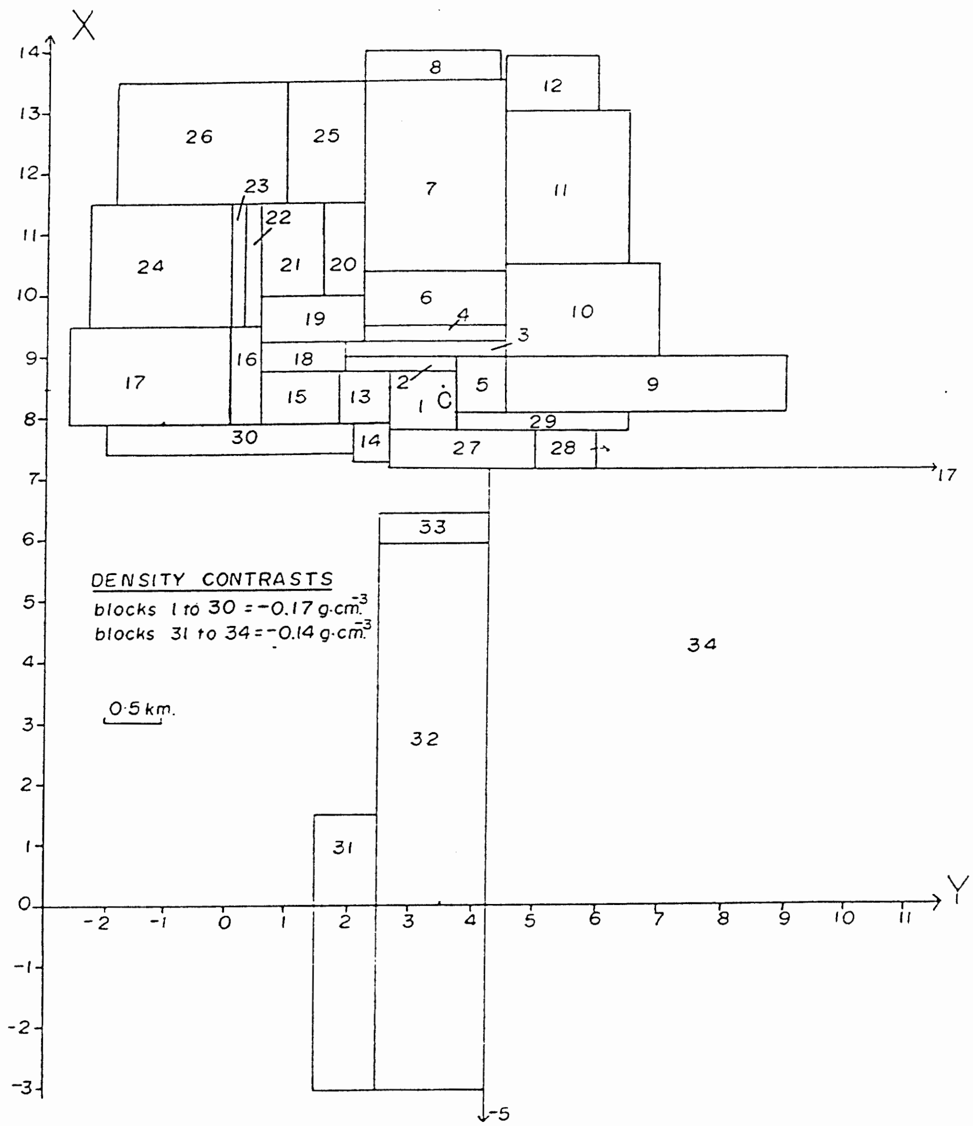

Figure 9. A schematic diagram showing a plan view of the blocks used to model the Liscomb Satellite Pluton and main Liscomb Complex.

To determine the effect of the main Liscomb Complex, several blocks approximating the complex were included in the modelling. Figure 9 shows a plan view of the study area and the location of the individual blocks. Blocks numbered 1 - 30 were used to approximate the subsurface mass distribution of the Liscomb Satellite Pluton using a density contrast of - 0.17 g/cm^3. Blocks numbered 30 - 34 were used as a rough approximation of the main Liscomb Complex, and the best- fitting density contrast of these blocks was - 0.14 g/cm^3. It was found that these density contrasts were required in order to fit the calculated and observed gravity values along the N-S' and NW-SE profiles.

Figure 10A shows the modelling results of the W-E profile of figure 6.

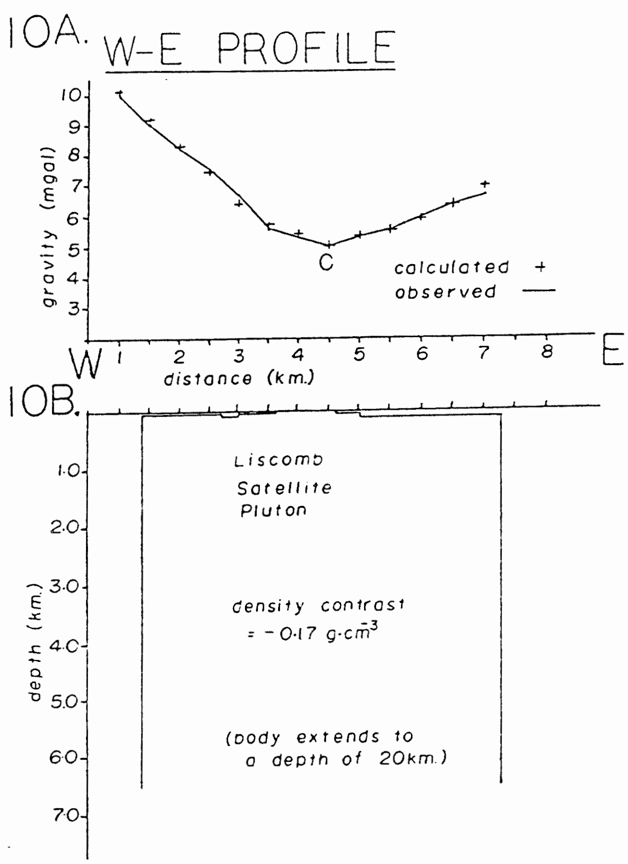

Figure 10. A schematic diagram showing the results of modelling using the program Threed along the W-E profile shown in figure 6.

Figure 10B shows a cross-section of the body along the W-E profile. The cross-section shows that the body slopes gently away from 'C' for a distance and then becomes nearly vertical. Figure 10B also shows that there is good agreement between the calculated values and the observed gravity values along the W-E profile.

The results of modelling along the N'-S' profile are shown in figure 11A.

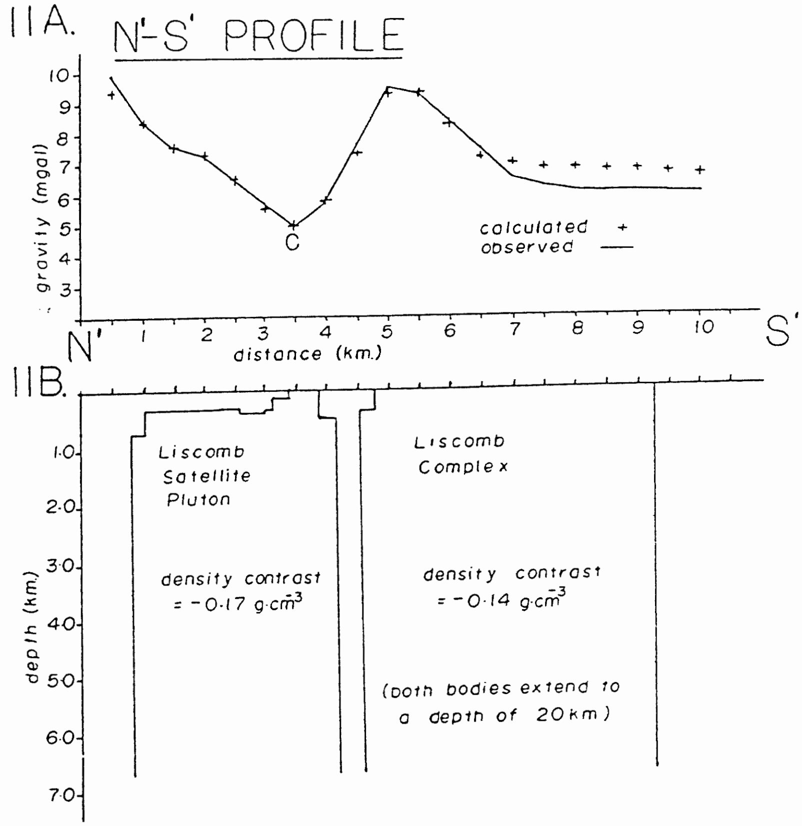

Figure 11. A schematic diagram showing the results of modelling using the program Threed along the N'-S' profile shown in figure 6.

Figure 11B shows the cross-sectional view underlying the N'-S' profile. Notable are the gently sloping northern contact of the satellite pluton, the steep southern contact, and the lack of a contact with the main Liscomb Complex along this profile. Figure 11A shows that good agreement exists between the calculated and observed gravity values along this profile except towards the southern end of the profile where the values calculated over the main Liscomb Complex are too high.

The program Threed only allows density values to be specified as integer values. Increasing the density contrast of the main Liscomb Complex to - 0.15 g/cm^3 produced too large anomaly. Modelling suggests that the density contrast of the main Liscomb Complex should be approximately - 0.143 g/cm^3. Unfortunately, the program Threed could not be modified to allow a density intermediate between -0.14 and -0.15 g/cm^3 to be used in the calculations.

Figure 12A shows the results of modelling along the NW-SE profile. Figure 12B shows a cross-section of the model along the NW-SE profile. Features of note are the gentle slope of the model to the northwest, and the connection between the pluton and the main Liscomb Complex. Modelling suggests that the minimim depth of the connection is 0.5 km.

The comparison between the calculated and observed gravity values along the NW-SE profile are shown in figure 12A. The fit between the values along the profile is good until the 5 km. station. Similar to the previous discussion involving the southern end of the N'-S' profile, a density contrast of - 0.14 g/cm^3 for the main Liscomb Complex does not produce a great enough anomaly to match the calculated and observed gravity values. As with the N'-S' profile, modelling suggests that a density contrast of - 0.143 g/cm^3 would be more appropriate for the blocks used to approximate the main Liscomb Complex.

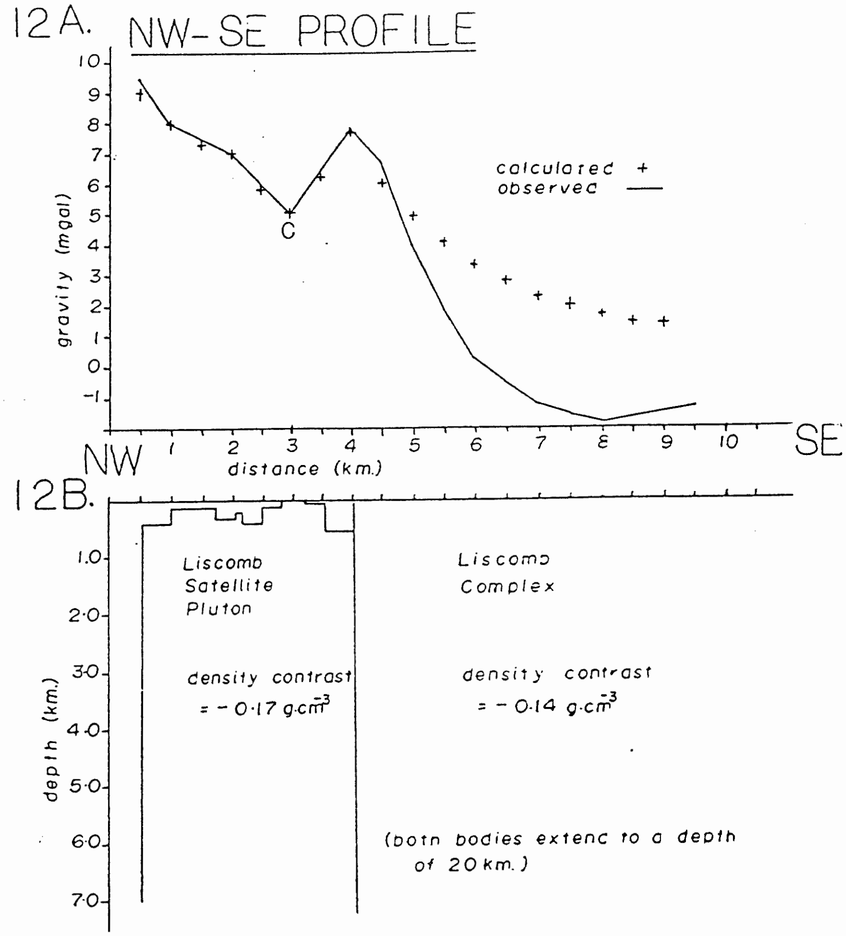

Figure 12. A schematic diagram showing the results of modelling using the program Threed along the NW-SE profile shown in figure 6.

To show the overall fit of the model produced using Threed a contour map of the calculated gravity values is presented in figure 13. Comparison between the calculated and observed gravity contours, in a general sense, show good agreement, especially in the area of the Liscomb Satellite Pluton and the northwest margin of the main Liscomb Complex. However, the observed gravity contours in the northeast area of figure 13 show that the Liscomb Satellite Pluton may extend further in this direction than the 3D model indicates. The observed contours also show that the main Liscomb Complex extends further to the northeast than allowed for in the modelling calculations. Similarily, the contours in the southwest corner of figure 13 indicate that the main Liscomb Complex extends further west in this area than the modelling accounted for in the calculations.

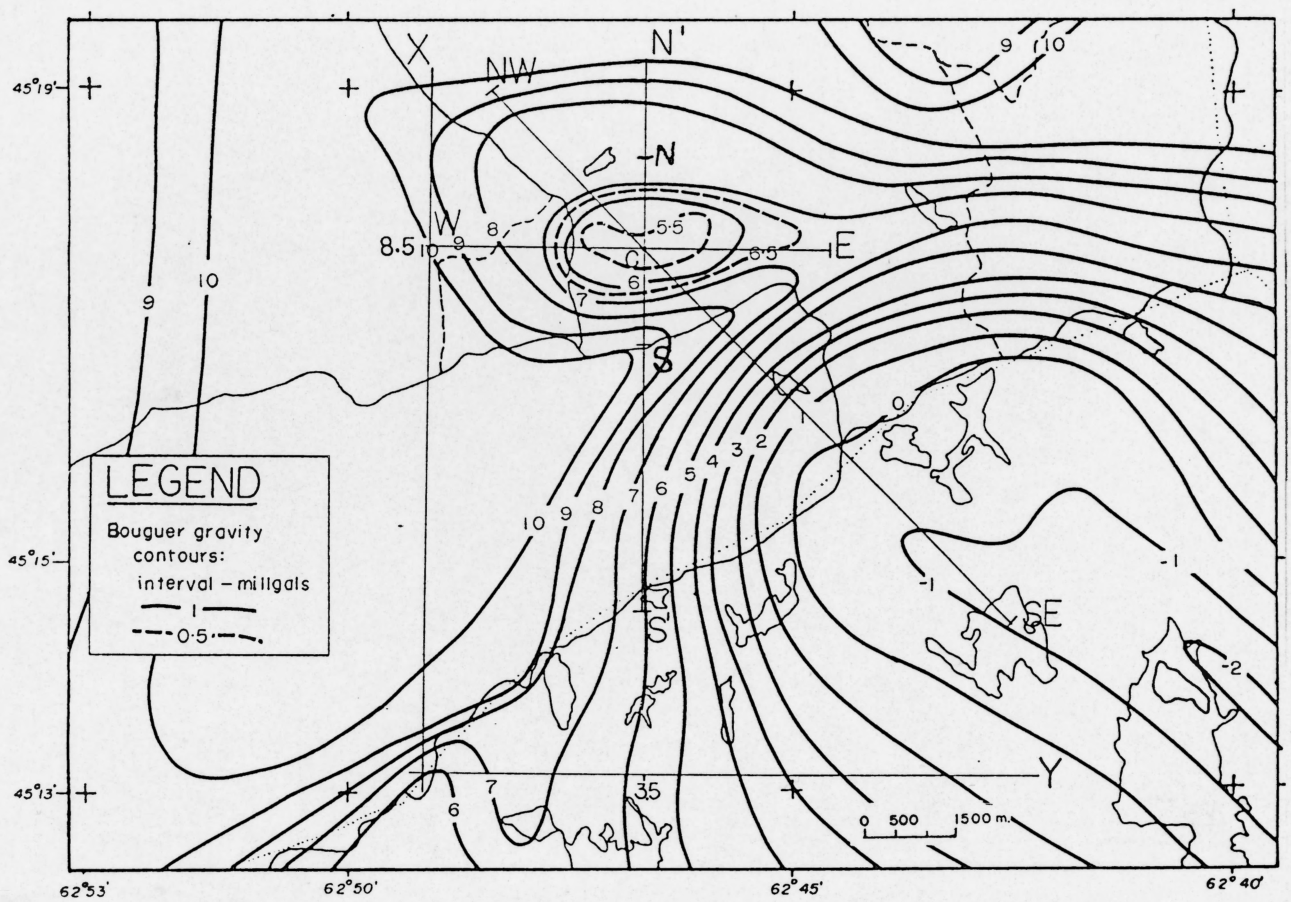

Figure 13. Schematic diagram comparing observed Bouguer anomaly with gravity values calculated for the model produced using the program Threed (overlay). To compare, unfold the white paper underlying the transparency.


LEGEND
calculated gravity
contours:
interval - milligals
1
0 500 1500m.

DISCUSSION

In the modelling process the density contrast functions as a scaling factor. A greater density contrast would decrease the overall dimensions of the model, whereas a smaller density contrast would have increased the overall dimensions of the model. In the program Magrav, the half-strike length parameter affects the model dimensions the same way as the density contrast. The calculations that are done by the Magrav program involve calculating the gravitational effect assumming the prism has infinite strike length and then subtracting the gravitational effect from the half-strike length value to infinity. Consequently, changing the half-strike length parameter changes the amount of mass used in the calculations.

The factor which controls the slope of the profile curves is the shape of the body. Because the Liscomb Satellite Pluton , and the main Liscomb Complex both outcrop depth to the top of the bodies was not a factor in this study. The anomaly magnitude is a function of the body and the density contrast.

To a first approximation, the body can be modelled as a subsurface finite length prism. However, this approximation will tend to minimize the depth extent and profile length of the bodies. The reason for this is that a uniform prism will introduce more mass at the corners of the body than may actually exist.

Model 1 produced using the Magrav program is a good first-order approximation and shows some interesting features: first, the steep slope of the contacts, especially the southern contact; and second, the lack of a contact with the main Liscomb

Complex along the N-S profile.

The 3D model produced using the Threed program shows that the Liscomb Satellite Pluton slopes gently to the west, east, and north away from point 'C' for a distance and then becomes nearly vertical. Similar to model 1, the 3D model also shows a steep southern margin. The overall geometry of the 3D model suggests that the pluton resembles an oval-shaped vertical cylinder with a convex upper surface. The 3D model suggests, however, that the satellite pluton may be connected to the main Liscomb Complex along the satellite pluton's southern margin, but only to the east of the point 'C'.

Model 1 shows that a density contrast of - 0.09 g/cm^3 is not sufficient to produce a calculated anomaly as large as the observed gravity anomaly. The 3D model indicates that a density contrast of - 0.17 g/cm^3 for the Liscomb Satellite Pluton, and a density contrast of - 0.14 g/cm^3 for the main Liscomb Complex can produce a large enough calculated anomaly to fit the observed gravity anomaly. However, 3D modelling suggests that a density contrast of - 0.143 g/cm^3 would allow a better fit between the calculated and observed gravity values in the area over the main Liscomb Complex. One effect of increasing the density contrast would be to increase the calculated depth to the top of the connection between the pluton and the complex.

The major problem with the models produced during this study concerns the density contrast used to model the bodies. On the basis of the local geology a value of - 0.09 g/cm^3 is actually a mean value based on Douma's (1978) data. The maximum density of the Halifax Slates is 2.95 g/cm^3 (Douma, 1978). The minimum density of granite is 2.61 g/cm^3 (Douma, 1978). If these values are accurate then a density contrast of - 0.17 g/cm^3 is a reasonable value.

P. Giles (personnal communication) has suggested that Halifax slates may actually separate the Liscomb Satellite pluton from the main Liscomb Complex. He bases his interpretation on aeromagnetic maps and outcrops of Halifax Slates to the west of the satellite pluton.

CONCLUSIONS

A high precision (± 0.05 mgal.) gravity survey conducted over the Liscomb Satellite Pluton shows a - 5.0 mgal. Bouguer anomaly centered over the pluton. Computer modelling of this anomaly has yielded a geologically feasible body. The body resembles an oval-shaped vertical cylinder with a convex upper surface. The body extends to a minimim depth of 20.0 km., the minimum north-south extent of the body is 3.5 km., and the minimum east-west extent of the body is 4.0 km. If the Liscomb Satellite Pluton is connected to the main Liscomb Complex, the connection has to be at a depth greater than 0.5 km.

REFERENCES

Bott, M.H. (1967): Gravity investigations of subsurface shape and mass distributions of granite batholiths, Geol. Soc. Am. Bull., vol. 78, p. 859 - 878.

Bujak, J. P. and Donohoe, H.V. Jr., (1980): Geological Highway Map of Nova Scotia; Atlantic Geoscience Society, Special Publication Number 1.

Clarke, D.B. and Halliday, A.N. (1980): Strontium isotope geology of the South Mountain Batholith, Nova Scotia; Geochimica et Cosmochimica Acta, vol. 44, p. 1045 - 1058; in Giles and Chatterjee, 1987.

Douma, M. (1978): Gravitational interpretation and modelling of the South Mountain Batholith; B.Sc. Honours Thesis, Dalhousie University.

Faribault, E.R. (1901, 1902): Geological map of the province of Nova Scotia, Halifax and Guysborough counties; in Giles and Chatterjee, 1987.

Garland, G.D. (1953): Gravity measurements in the Maritime Provinces; Publications of the Dominion Obs., vol. 16 (2), Dept. of Mines and Technical Surveys, p. 185 - 275.

Giles, P.S. and Chatterjee, A.K. (1986 - 1): New perspectives on granite-related mineral deposits in southern Nova Scotia; in Nova Scotia Department of Mines and Energy Report 87 - 1, p. 187 - 189.

Giles, P.S. and Chatterjee, A.K. (1986 - 2):Evolution of the Liscomb Complex and its relevance to metallogeny in the eastern Meguma Zone; in Nova Scotia Department of Mines and Energy Report 87 - 1, p. 191.

Giles, P.S. and Chatterjee, A.K. (1987): Peraluminous granites of the Liscomb Complex; in Nova Scotia Department of Mines and Energy Report 87 - 1, p. 95 - 98.

Nagy, D., (1966): The gravitional attraction of a right rectangular prism; Geophysics, Vol. 31 (2), p. 363 - 371.

O'Reilly, C.T. (1975): Gravitational interpretation and modelling of the South Mountain Batholith, utilizing two and three dimensional computer programming; B.Sc. Honours Thesis, Dalhousie University.

Reynolds, P.H. and Muecke, G.K. (1978): Age studies on slates: Applicability of the 40Ar / 39Ar stepwise outgassing method; Earth and Planetary Science Letters, Vol. 40, p. 111 - 118.

Smith, R.A. (1959):Some depth formulae for local magnetic and gravity anomalies; Geophys. Prosp., vol. 7, p. 55 - 63.

Talwani, M., Worzel, J.L., and Landisman, M. (1959): Rapid gravity computations for two-dimensional bodies with application for the Mendocino Fracture Zone; J. Geophys. Res., vol. 64, p. 49 - 59.

Telford, W., Geldart, L., Sheriff, R., and Key, S. (1976): Applied Geophysics. Cambridge University Press, New York, 860p.

APPENDIX A

UNITS: m = metre
min = minutes
div = divisions
mgal = millgals

LINE DESCRIPTION (reference to figure 4):

Powerline - Starts at station 11910 and extends SW to station 19442.
Line 1 - Starts at station 1A and extends south to Station 7A.
Line 2 - Starts at station 1 and extends north to station 6.
Line 3 - Starts at station 1 (fourth station from southend of Line 4) and extends south along road to base station.
Line 4 - Starts at station 0N (fifth station from southend of Line 4) and extends north to station 7N and then west to station 18N.
Line 5 - Starts at station 0E on road and extends east to 10E and north from 6E to 11E-N.
Line 6 - Starts at station 0S (northern most station on line 6) and extends south to station 10S north of road. then starts again at station 0NS (southern most station on line 6) and extends north to station 3NS just south of the road.

STATION	DIST (m)	EL (m)	T_cor (div)	t (min)	READ (div)	B_COR (div)	C_READ (div)	G_OBS (mgal)	D_COR (mgal)	L_COR (mgal)	D_EL (m)	F_B_COR (mgal)	B_GRAV (mgal)	EMR_C (mgal)	COMMENTS
BASE STN	0.0	198.000	0.000	0	4078.860	0.000	4078.860	4315.125	0.000	0.000	0.000	0.000	0.00	-9.73	- Powerline
11910	2779.0	147.850	0.000	60	4095.520	0.000	4095.520	4332.790	0.040	-2.270	-50.150	-9.679	5.76	-3.97	- Powerline
11909	2668.0	151.600	0.000	75	4094.850	0.000	4094.850	4332.079	0.050	-2.180	-46.400	-8.955	5.87	-3.86	- Powerline
C	1567.0	178.000	0.215	123	4084.270	0.000	4084.485	4321.089	0.081	-1.280	-20.000	-3.860	0.91	-8.82	- Powerline
B	1346.0	197.000	0.420	131	4079.480	0.000	4079.900	4316.228	0.087	-1.100	-1.000	-0.193	-0.10	-9.83	- Powerline
11907	820.0	194.300	0.210	150	4079.660	0.000	4079.870	4316.196	0.099	-0.670	-3.700	-0.714	-0.21	-9.94	- Powerline
11906	599.8	195.250	0.080	179	4079.555	0.000	4079.635	4315.947	0.118	-0.490	-2.750	-0.531	-0.08	-9.81	- Powerline
BASE STN	0.0	198.000	0.070	192	4078.670	0.000	4078.740	4314.998	0.127	0.000	0.000	0.000	0.00	-9.73	- Powerline
19442	-5998.0	194.170	0.035	231	4080.790	0.000	4080.825	4317.209	0.103	4.900	-3.830	-0.739	6.35	-3.38	- Powerline
9994	-5949.0	206.610	0.000	243	4078.090	0.000	4078.090	4314.309	0.096	4.860	8.610	1.662	5.80	-3.93	- Powerline
9995	-5777.0	215.040	0.000	254	4076.455	0.000	4076.455	4312.575	0.089	4.720	17.040	3.289	5.55	-4.18	- Powerline
9996	-5655.0	214.660	0.000	266	4076.435	0.000	4076.435	4312.554	0.082	4.620	16.660	3.215	5.35	-4.38	- Powerline
9997	-5018.0	205.740	0.000	281	4079.775	0.000	4079.775	4316.095	0.073	4.100	7.740	1.494	6.64	-3.09	- Powerline
9998	-4027.0	211.590	0.000	319	4081.205	0.000	4081.205	4317.612	0.051	3.290	13.590	2.623	8.45	-1.28	- Powerline
9999	-2900.0	206.590	0.000	350	4082.450	0.000	4082.450	4318.932	0.031	2.370	8.590	1.658	7.87	-1.86	- Powerline
11900	-2754.0	209.490	0.000	374	4081.500	0.000	4081.500	4317.924	0.016	2.250	11.490	2.218	7.28	-2.45	- Powerline
11901	-2154.0	203.820	0.000	396	4081.225	0.000	4081.225	4317.633	0.002	1.760	5.820	1.123	5.39	-4.34	- Powerline
BASE STN	0.0	198.000	0.000	418	4078.870	0.000	4078.870	4315.136	-0.011	0.000	0.000	0.000	0.00	-9.73	- Powerline
BASE STN	0.0	198.000	0.000	0	4078.875	-0.015	4078.860	4315.125	0.000	0.000	0.000	0.000	0.00	-9.73	- Powerline
11903	-1395.0	211.630	0.000	30	4075.800	-0.015	4075.785	4311.865	-0.056	1.140	13.630	2.631	0.46	-9.27	- Powerline
A	-845.0	204.000	0.000	60	4076.580	-0.015	4076.565	4312.692	-0.111	0.690	6.000	1.158	-0.70	-10.43	- Powerline
11905	-526.0	220.790	0.000	81	4073.650	-0.015	4073.635	4309.585	-0.151	0.430	22.790	4.398	-0.86	-10.59	- Powerline
BASE STN	0.0	198.000	0.000	235	4079.020	-0.015	4079.005	4315.279	-0.154	0.000	0.000	0.000	0.00	-9.73	- Line 1
1A	6744.0	198.000	0.000	261	4092.495	-0.015	4092.480	4329.567	-0.167	-5.510	0.000	0.000	8.76	-0.97	- Line 1
2A	6328.0	189.000	0.000	266	4093.430	-0.015	4093.415	4330.558	-0.170	-5.170	-9.000	-1.737	8.36	-1.37	- Line 1
3A	6328.0	196.000	0.000	272	4092.005	-0.015	4091.990	4329.047	-0.173	-5.170	-2.000	-0.386	8.19	-1.54	- Line 1

4A	6230.0	171.000	0.000	276	4096.410	-0.015	4096.395	4333.718	-0.175	-5.090	-27.000	-5.211	8.12	-1.61	- Line 1
5A(E)	4847.0	179.000	0.000	283	4095.815	-0.015	4095.800	4333.087	-0.178	-3.960	-19.000	-3.667	10.16	0.43	- Line 1
6A	3966.0	164.000	0.000	288	4094.790	-0.015	4094.775	4332.000	-0.181	-3.240	-34.000	-6.562	6.89	-2.84	- Line 1
7A	2754.0	156.000	0.000	296	4092.350	-0.015	4092.335	4329.413	-0.185	-2.250	-42.000	-8.106	3.75	-5.98	- Line 1
BASE STN	0.0	198.000	0.000	318	4079.060	-0.015	4079.045	4315.321	-0.196	0.000	0.000	0.000	0.00	-9.73	- Line 1
BASE STN	0.0	198.000	0.000	94	4079.040	-0.015	4079.025	4315.300	-0.175	0.000	0.000	0.000	0.00	-9.73	- Line 2
1	1824.0	202.000	0.000	111	4087.980	-0.015	4087.965	4324.779	-0.172	-1.490	4.000	0.772	8.76	-0.97	- Line 2
2A	3023.0	226.000	0.000	125	4081.590	-0.015	4081.575	4318.004	-0.170	-2.470	28.000	5.404	5.64	-4.09	- Line 2
3	4027.0	189.000	0.000	137	4090.640	-0.015	4090.625	4327.600	-0.169	-3.290	-9.000	-1.737	7.28	-2.45	- Line 2
4	4970.0	209.000	0.000	147	4088.430	-0.015	4088.415	4325.256	-0.167	-4.060	11.000	2.123	8.03	-1.70	- Line 2
5	5178.0	217.000	0.000	153	4088.470	-0.015	4088.455	4325.299	-0.166	-4.230	19.000	3.667	9.45	-0.28	- Line 2
6	5802.0	217.000	0.000	159	4090.924	-0.015	4090.909	4327.901	-0.165	-4.740	19.000	3.667	11.54	1.81	- Line 2
BASE STN	0.0	198.000	0.000	0	4079.110	-0.250	4078.860	4315.125	0.000	0.000	0.000	0.000	0.00	-9.73	- Line 3
1	2650.0	206.042	0.000	11	4086.580	-0.250	4086.330	4323.046	-0.006	-2.165	8.042	1.552	7.30	-2.43	- Line 3
2	2600.0	211.825	0.000	19	4085.540	-0.250	4085.290	4321.943	-0.010	-2.124	13.825	2.668	7.35	-2.38	- Line 3
3	2525.0	217.557	0.000	26	4084.640	-0.250	4084.390	4320.989	-0.014	-2.063	19.557	3.775	7.56	-2.17	- Line 3
4	2425.0	222.680	0.000	31	4083.750	-0.250	4083.500	4320.045	-0.017	-1.981	24.680	4.763	7.69	-2.04	- Line 3
5	2525.0	207.614	0.000	37	4086.595	-0.250	4086.345	4323.062	-0.020	-2.063	9.614	1.856	7.71	-2.02	- Line 3
6	2525.0	213.059	0.000	42	4085.445	-0.250	4085.195	4321.842	-0.023	-2.063	15.059	2.906	7.54	-2.19	- Line 3
7A	2425.0	212.472	0.000	47	4085.005	-0.250	4084.755	4321.376	-0.026	-1.981	14.472	2.793	7.04	-2.69	- Line 3
7	2375.0	212.407	0.000	63	4084.565	-0.250	4084.315	4320.909	-0.035	-1.940	14.407	2.781	6.59	-3.14	- Line 3
8	2125.0	209.406	0.000	70	4083.715	-0.250	4083.465	4320.008	-0.038	-1.736	11.406	2.201	5.31	-4.42	- Line 3
9	2025.0	209.491	0.000	78	4083.430	-0.250	4083.180	4319.706	-0.043	-1.654	11.491	2.218	5.10	-4.63	- Line 3
10	1850.0	210.637	0.000	85	4082.180	-0.250	4081.930	4318.380	-0.047	-1.511	12.637	2.439	4.14	-5.59	- Line 3
11	1725.0	208.383	0.000	95	4081.875	-0.250	4081.625	4318.057	-0.052	-1.409	10.383	2.004	3.48	-6.25	- Line 3
12	1575.0	210.486	0.000	98	4080.900	-0.250	4080.650	4317.023	-0.054	-1.287	12.486	2.410	2.97	-6.76	- Line 3
13	1250.0	215.316	0.000	108	4078.840	-0.250	4078.590	4314.839	-0.059	-1.021	17.316	3.342	1.98	-7.75	- Line 3
14	950.0	218.171	0.000	115	4077.515	-0.250	4077.265	4313.434	-0.063	-0.776	20.171	3.893	1.36	-8.37	- Line 3
15	750.0	215.413	0.000	123	4077.410	-0.250	4077.160	4313.323	-0.067	-0.613	17.413	3.361	0.88	-8.85	- Line 3
BASE STN	0.0	198.000	0.000	135	4079.180	-0.250	4078.930	4315.199	-0.074	0.000	0.000	0.000	0.00	-9.73	- Line 3
BASE STN	0.0	198.000	0.000	0	4079.150	-0.290	4078.860	4315.125	0.000	0.000	0.000	0.000	0.00	-9.73	- Line 4
0N	2650.0	206.042	0.000	0	4086.580	-0.290	4086.290	4323.003	0.000	-2.165	8.042	1.552	7.26	-2.47	- Line 4
1N	2875.0	206.960	0.000	20	4086.195	-0.290	4085.905	4322.595	0.000	-2.349	8.960	1.729	6.85	-2.88	- Line 4
2N	2950.0	209.838	0.000	27	4085.520	-0.290	4085.230	4321.879	0.000	-2.410	11.838	2.285	6.63	-3.10	- Line 4
3N	3100.0	202.478	0.000	35	4086.800	-0.290	4086.510	4323.237	0.000	-2.532	4.478	0.864	6.44	-3.29	- Line 4
4N	3175.0	199.725	0.000	47	4087.255	-0.290	4086.965	4323.719	0.000	-2.594	1.725	0.333	6.33	-3.40	- Line 4
5N	3275.0	196.022	0.000	59	4087.815	-0.290	4087.525	4324.313	0.000	-2.675	-1.978	-0.382	6.13	-3.60	- Line 4
6N	3350.0	194.254	0.000	64	4088.090	-0.290	4087.800	4324.604	0.000	-2.737	-3.746	-0.723	6.02	-3.71	- Line 4
7N	3475.0	193.980	0.000	70	4087.930	-0.290	4087.640	4324.435	0.000	-2.839	-4.020	-0.776	5.70	-4.03	- Line 4
8N	3450.0	193.482	0.000	75	4088.110	-0.290	4087.820	4324.626	0.000	-2.818	-4.518	-0.872	5.81	-3.92	- Line 4
9N	3400.0	202.708	0.000	82	4086.350	-0.290	4086.060	4322.759	0.000	-2.777	4.708	0.909	5.77	-3.96	- Line 4
10N	3350.0	210.153	0.000	88	4085.030	-0.290	4084.740	4321.360	0.000	-2.737	12.153	2.346	5.84	-3.89	- Line 4
11N	3325.0	208.212	0.000	93	4085.420	-0.290	4085.130	4321.773	0.000	-2.716	10.212	1.971	5.90	-3.83	- Line 4
12N	3475.0	213.253	0.000	99	4084.135	-0.290	4083.845	4320.411	0.000	-2.839	15.253	2.944	5.39	-4.34	- Line 4
13N	3500.0	213.764	0.000	103	4083.930	-0.290	4083.640	4320.193	0.000	-2.859	15.764	3.042	5.25	-4.48	- Line 4
14N	3550.0	208.871	0.000	110	4084.800	-0.290	4084.510	4321.116	0.000	-2.900	10.871	2.098	5.19	-4.54	- Line 4
15N	3550.0	204.253	0.000	116	4085.585	-0.290	4085.295	4321.948	0.000	-2.900	6.253	1.207	5.13	-4.60	- Line 4
16N	3550.0	215.176	0.000	121	4083.560	-0.290	4083.270	4319.801	0.000	-2.900	17.176	3.315	5.09	-4.64	- Line 4
17N	3575.0	213.421	0.000	126	4083.890	-0.290	4083.600	4320.151	0.000	-2.920	15.421	2.976	5.08	-4.65	- Line 4
18N	3475.0	210.353	0.000	132	4084.720	-0.290	4084.430	4321.031	0.000	-2.839	12.353	2.384	5.45	-4.28	- Line 4
BASE STN	0.0	198.000	0.000	150	4079.150	-0.290	4078.860	4315.125	0.000	0.000	0.000	0.000	0.00	-9.73	- Line 4
BASE STN	0.0	198.000	0.000	0	4079.150	-0.290	4078.860	4315.125	0.000	0.000	0.000	0.000	0.00	-9.73	- Line 5
0E	3450.0	215.000	0.045	160	4085.380	-0.290	4085.135	4321.779	-0.739	-2.818	17.000	3.281	6.38	-3.35	- Line 5
1E	3425.0	220.466	0.105	151	4083.595	-0.290	4083.410	4319.950	-0.698	-2.798	22.466	4.336	5.66	-4.07	- Line 5
2E	3425.0	221.367	0.155	147	4083.280	-0.290	4083.145	4319.669	-0.679	-2.798	23.367	4.510	5.58	-4.15	- Line 5

3E	3425.0	220.252	0.205	142	4083.345	-0.290	4083.260	4319.791	-0.656	-2.798	22.252	4.295	5.51	-4.22	-	Line 5
4E	3425.0	220.657	0.340	129	4082.625	-0.290	4082.675	4319.170	-0.596	-2.798	22.657	4.373	5.02	-4.71	-	Line 5
5E	3425.0	221.238	0.425	123	4082.460	-0.290	4082.595	4319.085	-0.568	-2.798	23.238	4.485	5.08	-4.65	-	Line 5
6E	3300.0	222.322	0.740	93	4082.120	-0.290	4082.570	4319.059	-0.430	-2.696	24.322	4.694	5.50	-4.23	-	Line 5
8E	3300.0	223.610	0.545	113	4081.910	-0.290	4082.165	4318.630	-0.522	-2.696	25.610	4.943	5.23	-4.50	-	Line 5
9E	3425.0	222.026	0.610	108	4082.140	-0.290	4082.460	4318.942	-0.499	-2.798	24.026	4.637	5.16	-4.57	-	Line 5
10E	3425.0	222.454	0.675	101	4082.005	-0.290	4082.390	4318.868	-0.467	-2.798	24.454	4.720	5.20	-4.53	-	Line 5
7E-N	3425.0	221.630	0.780	85	4082.225	-0.290	4082.715	4319.213	-0.393	-2.798	23.630	4.561	5.46	-4.27	-	Line 5
8E-N	3575.0	215.270	0.805	79	4083.445	-0.290	4083.960	4320.533	-0.365	-2.920	17.270	3.333	5.46	-4.27	-	Line 5
9E-N	3725.0	207.725	0.825	73	4084.950	-0.290	4085.485	4322.150	-0.337	-3.043	9.725	1.877	5.52	-4.21	-	Line 5
10E-N	3850.0	208.561	0.845	63	4085.025	-0.290	4085.580	4322.250	-0.291	-3.145	10.561	2.038	5.73	-4.00	-	Line 5
11E-N	4200.0	188.563	0.855	55	4089.565	-0.290	4090.130	4327.075	-0.254	-3.431	-9.437	-1.821	6.44	-3.29	-	Line 5
BASE STN	0.0	198.000	0.035	179	4079.895	-0.290	4079.640	4315.952	-0.827	0.000	0.000	0.000	0.00	-9.73	-	Line 5
BASE_STN	0.0	198.000	0.000	0	4080.065	-1.205	4078.860	4315.125	0.000	0.000	0.000	0.000	0.00	-9.73	-	Line 6
0S	4010.0	180.856	0.000	26	4093.440	-1.205	4092.235	4329.307	0.011	-3.276	-17.144	-3.309	7.61	-2.12	-	Line 6
1S	3880.0	182.106	0.000	33	4092.925	-1.205	4091.720	4328.761	0.014	-3.169	-15.894	-3.068	7.41	-2.32	-	Line 6
2S	3760.0	190.137	0.000	40	4091.200	-1.205	4089.995	4326.932	0.017	-3.071	-7.863	-1.518	7.23	-2.50	-	Line 6
3S	3620.0	199.471	0.000	51	4089.270	-1.205	4088.065	4324.885	0.022	-2.957	1.471	0.284	7.11	-2.62	-	Line 6
4S	3490.0	204.688	0.000	61	4088.130	-1.205	4086.925	4323.677	0.026	-2.851	6.688	1.291	7.02	-2.71	-	Line 6
5S	3340.0	202.299	0.000	70	4087.970	-1.205	4086.765	4323.507	0.030	-2.728	4.299	0.830	6.51	-3.22	-	Line 6
6S	3200.0	199.319	0.000	78	4088.360	-1.205	4087.155	4323.920	0.033	-2.614	1.319	0.255	6.47	-3.26	-	Line 6
7S	3050.0	201.403	0.000	85	4087.920	-1.205	4086.715	4323.454	0.036	-2.491	3.403	0.657	6.53	-3.20	-	Line 6
8S	2910.0	199.993	0.000	92	4088.325	-1.205	4087.120	4323.883	0.039	-2.377	1.993	0.385	6.80	-2.93	-	Line 6
9S	2750.0	205.463	0.000	100	4087.570	-1.205	4086.365	4323.083	0.043	-2.246	7.463	1.440	7.19	-2.54	-	Line 6
10S	2650.0	208.353	0.000	108	4087.150	-1.205	4085.945	4322.637	0.046	-2.165	10.353	1.998	7.39	-2.34	-	Line 6
D	1870.0	246.338	0.000	128	4080.890	-1.205	4079.685	4316.000	0.055	-1.528	48.338	9.329	8.73	-1.00	-	
E	1470.0	230.238	0.000	137	4085.140	-1.205	4083.935	4320.506	0.059	-1.201	32.238	6.222	10.46	0.73	-	
0NS	1760.0	219.576	0.000	156	4082.830	-1.205	4081.625	4318.057	0.067	-1.438	21.576	4.164	5.72	-4.01	-	Line 6
1NS	1980.0	216.261	0.000	165	4084.645	-1.205	4083.440	4319.981	0.071	-1.617	18.261	3.524	6.83	-2.90	-	Line 6
2NS	2100.0	214.480	0.000	175	4085.480	-1.205	4084.275	4320.867	0.075	-1.715	16.480	3.181	7.28	-2.45	-	Line 6
3NS	2330.0	211.173	0.000	184	4086.310	-1.205	4085.105	4321.747	0.079	-1.903	13.173	2.542	7.34	-2.39	-	Line 6
BASE_STN	0.0	198.000	0.000	198	4079.985	-1.205	4078.780	4315.040	0.085	0.000	0.000	0.000	0.00	-9.73	-	Line 6